ornl



ORNL/TM-7117

OAK
RIDGE
NATIONAL
LABORATORY

UNION
CARBIDE

# Kinetics of Silica Deposition from Simulated Geothermal Brines

E. G. Bohlmann
R. E. Mesmer
P. Berlinski

OPERATED BY
UNION CARBIDE CORPORATION
FOR THE UNITED STATES
DEPARTMENT OF ENERGY

## DISCLAIMER

Printed in the United States of America. Available from
National Technical Information Service
U.S. Department of Commerce
5285 Port Royal Road, Springfield, Virginia 22161
NTIS price codes—Printed Copy: A03 Microfiche A01

ORNL/TM-7117
UC-4 Chemistry

Contract No. W-7405-eng-26

CHEMISTRY DIVISION

# KINETICS OF SILICA DEPOSITION FROM SIMULATED GEOTHERMAL BRINES

E. G. Bohlmann, R. E. Mesmer, P. Berlinski

Date Published: March 1980



**NOTICE** This document contains information of a preliminary nature. *It is subject to revision or correction and therefore does not represent a* final report.

OAK RIDGE NATIONAL LABORATORY
Oak Ridge, Tennessee 37830
operated by
UNION CARBIDE CORPORATION
for the
DEPARTMENT OF ENERGY

CONTENTS

## SUMMARY

In our experiments supersaturated brines were passed through columns packed with several forms of silica (crystalline α quartz, polycrystalline α quartz, and porous Vycor). Also, silica deposition on $ThO_2$ microspheres and titanium powder was studied under controlled conditions of supersaturation, pH, temperature, and salinity. The residence time was varied by adjustments of flow rate and column length. The silica contents of the input and effluent solutions were determined colorimetrically by a molybdate method which does not include polymers without special pretreatment.

The following observations have been made:

(1) Essentially identical deposition behavior was observed once the substrate was thoroughly coated with amorphous silica and the BET surface area of the coated particles was taken into account.

(2) The reaction rate is not diffusion limited in the columns.

(3) The silica deposition is a function of the monomeric ($Si(OH)_4$) concentration in the brine.

(4) The deposition on all surfaces examined was spontaneously nucleated.

(5) The dependence on the supersaturation concentration, hydroxide ion concentration, surface area, temperature and salinity were examined. Fluoride was shown to have no effect at pH 5.94 and low salinity.

The empirical rate law which describes our data in 1 m NaCl in the pH range 5-7 and temperatures from 60-120°C is:

$$-\frac{d[Si(OH)_4]}{dt} = 0.12\ A\ ([Si(OH)_4] - [Si(OH)_4]_{eq})^2\ [OH^-]^{0.7} \qquad (1)$$

where A is the surface area in $cm^2$ amorphous $SiO_2$ per kg of water in column voids, t is in minutes, and the concentrations are in molal units. Hydroxide concentration was derived from the measured pH and the ionization quotient for water. In the expression given above the rate constant

is essentially independent of temperature over the range 60-120°C. A cursory study of the effect of salinity showed little difference for 0.09 and 1.0 m NaCl solutions; however, increasing the concentration to 4.0 m increased the deposition rate by more than an order of magnitude. The rate of linear growth of an amorphous silica surface in cm/min in $\leq$ 1 m NaCl is given by

$$\frac{dh}{dt} = 3.1\ ([Si(OH)_4] - [Si(OH)_4]_{eq})^2\ [OH^-]^{0.7} \qquad (2)$$

These equations can be used to estimate the rate at which reinjection formations will plug given data on the porosity, area, and brine pH and monomeric silica concentration. Experience with various substrates indicates they all become coated with amorphous silica in relatively short times even in the absence of amorphous silica-like materials. Deposition then proceeds according to the rate equations given.

# 1. INTRODUCTION

## 1.1 General (Behavior of Silica)

The principal materials[1,2] deposited from geothermal brines as the heat is extracted are $CaCO_3$, metal sulfides, and amorphous silica or mixed phases in an amorphous matrix. The deposition of calcium carbonate is rapid when supersaturation conditions exist as a result of the removal of $CO_2$. When the brines are extracted from deep hot reservoirs, the silica content corresponds to the solubility of α quartz in the brine at the reservoir temperature.[3] Because of the very slow kinetics of crystallization of quartz below 300°C, silica is deposited during the heat extraction process as the more soluble amorphous form. Deposition may occur in well casings, piping, valves, flash tanks - where concentrations and the degree of supersaturation are increased - in heat exchangers, on turbine blades, in holdup storage ponds or in subsurface formations where fluids are reinjected for disposal. The latter is a serious threat to the lifetime of the reinjection well since maintenance of the porosity and permeability of the formation in the vicinity of the well bore are critical factors.

The mode of occurrence of silica in dilute aqueous solutions is generally accepted to be as the species $Si(OH)_4$ in the acidic-to-neutral pH range. In basic solutions the anionic species $SiO(OH)_3^-$, $SiO_2(OH)_2^{2-}$, and $Si_4(OH)_{18}^{2-}$ have been observed[4,5] in potentiometric studies. The equilibrium reactions amongst these anions and the neutral silicic acid have been studied in detail in sodium chloride solutions to 300°C. Also, the fluoride ion interacts with silicic acid in relatively acidic solutions, producing principally the $SiF_6^{2-}$ complex.[6] The stability of the complex decreases as the temperature increases.

The solubility in water of the most rapidly precipitating solid form, amorphous silica, has been investigated by Fournier to 350°C.[7] The solubility to 250°C at the saturation vapor pressure is represented in molal units by the expression

$$\log [Si(OH)_4] = -0.26 - 731/T \qquad (1)$$

It is generally accepted that in equilibrium with amorphous silica (and also for the more insoluble crystalline phases of silica - quartz, crystobalite, etc.) the principal silica present in acidic solutions is monomeric silicic acid. This is based on the rapid color development in the molybdate method of analysis and also on analysis of potentiometric data in nearly saturated solutions.[4,5] However, when the solution phase is supersaturated with respect to amorphous silica, polymerization proceeds with formation of colloidal particles and ultimately amorphous silica precipitates. The most regularly formed amorphous silica is natural opal consisting of a lattice-like structure of primary and secondary spheres.[8]

The polymerization process has been studied extensively and there is now considerable information on the nucleation process and the initial stages of polymer growth, but insufficient information exists to permit an analytical description of the growth process from homogeneous solution onto preformed surfaces. It was the objective of this present work to conduct laboratory studies which would provide such kinetic information applicable to deposition in formations used for waste brine disposal by reinjection and on in-plant equipment during heat extraction. Previous workers[9-17] have extensively investigated silica polymerization from supersaturated solutions with widely disparate results depending on the particular experimental conditions. Reaction orders vary from 0 to 8, with induction periods of varying duration observed. Widely varying colloids, precipitates and deposits are formed. The lack of reproducibility, of course, stems from the large number of factors affecting the polymerization process, as has been demonstrated by these studies: method used to prepare supersaturated solutions, pH, solution concentration and composition ($Cl^-$, $F^-$), temperature, hydrodynamics, impurities which act as active nuclei, analytical procedures, and combinations of these. The vagaries of the nucleation process which initiates polymeric growth are a substantial complication to the prediction of silica deposition in geothermal applications. On the premise that geothermal brines would be well supplied with nucleation promoters and that reinjection formations would provide sites for initiating

silica deposition, we undertook to study the growth kinetics of silica deposition on seeded or coated substrates. The work was part of a program at Oak Ridge National Laboratory to examine silica deposition behavior in dynamic geothermal systems from hydrothermal brines which are found in the western United States.

## 1.2 Kinetics of Crystal Growth

The theory of crystal growth is not yet at a stage where the mechanism of growth or the form of kinetic rate law are predictable[18,19,20] unless the process is under diffusion control. The growth rate for some substances is indeed limited by diffusion in solution, but for others it is limited by interface reactions. Since in the case of silica deposition the process is accompanied by dehydration, one might expect interface reaction limitation.

Fick's first law of diffusion describes the heterogeneous processes which are diffusion limited, i.e.,

$$J = - D \frac{\Delta \underline{m}}{\Delta X} A \qquad (2)$$

where J is the flux of deposition (moles $kg^{-1}$ $sec^{-1}$ $cm^{-2}$), $\Delta \underline{m}$ is the change in concentration across the film of thickness $\Delta X$ and A is the surface area per kilogram of water.

Where interface reactions are limiting the form commonly observed is

$$- \frac{d\underline{m}}{dt} = kA \, (\underline{m} - \underline{m}_e)^n \qquad (3)$$

where k is a specific rate constant, A is the area of the solid per kg of solution and $\underline{m}_e$ represents the molal solubility of the substance. The order of the reaction depends on the number of ions involved in the formula of the salt. There is not yet a very satisfactory explanation for this mathematical form with respect to the concentrations, but the most often quoted one was put forth by Doremus.[21] In his work on ionic salts, n took values of 3 and 4 depending on the number of ions in the crystal. The essential part of his detailed interpretation is that the rate limiting step involves adsorption of the reacting species on the

surface and that this adsorption is proportional to the difference $\underline{m} - \underline{m}_e$.

## 2. EXPERIMENTAL

### 2.1 Apparatus

The brine preparation and packed column setup are shown in Fig. 1. Brine of appropriate composition was pumped through a preheater and saturator column with the column held at the temperature required to give the desired silica concentration. The silica saturated brine thus prepared then passed through a manifold held at the same or a slightly higher temperature to prevent premature polymerization; a sampling station provided for monitoring the silica concentration in the brine. Connections from the manifold to the packed columns and their individual effluent samplers were made with titanium capillary tubing and minimum holdup valves to minimize extraneous volumes. The columns and a temperature adjustment coil were immersed in thermostatted baths as shown. Initially the columns were 9.5 mm I.D. Pyrex pipe, but later 8.4 mm I.D. titanium pipe was used. The effluent was quenched in a capillary coil in an ice bath; our experience has shown this to be an effective way to prevent capillary and valve plugging. The samples were taken in volumetric flasks containing an aliquot of hydrochloric acid solution such that the pH of the mixture was between 2 and 3; supersaturated silica brines such as we have dealt with are stable for hours in this pH range.

### 2.2 The Packed Column Approach

In this program we have packed small columns with various substrates of known BET surface areas and then passed solutions supersaturated with silica to coat the substrates with amorphous silica. Then we examined the kinetics of deposition on the coated surfaces and measured the BET surface areas when the experiment was completed.

The use of a packed column has several advantages in studies of this type. The principal advantages are:

(1) The high surface area-to-volume ratio which allows the deposition on the bed to occur to the exclusion

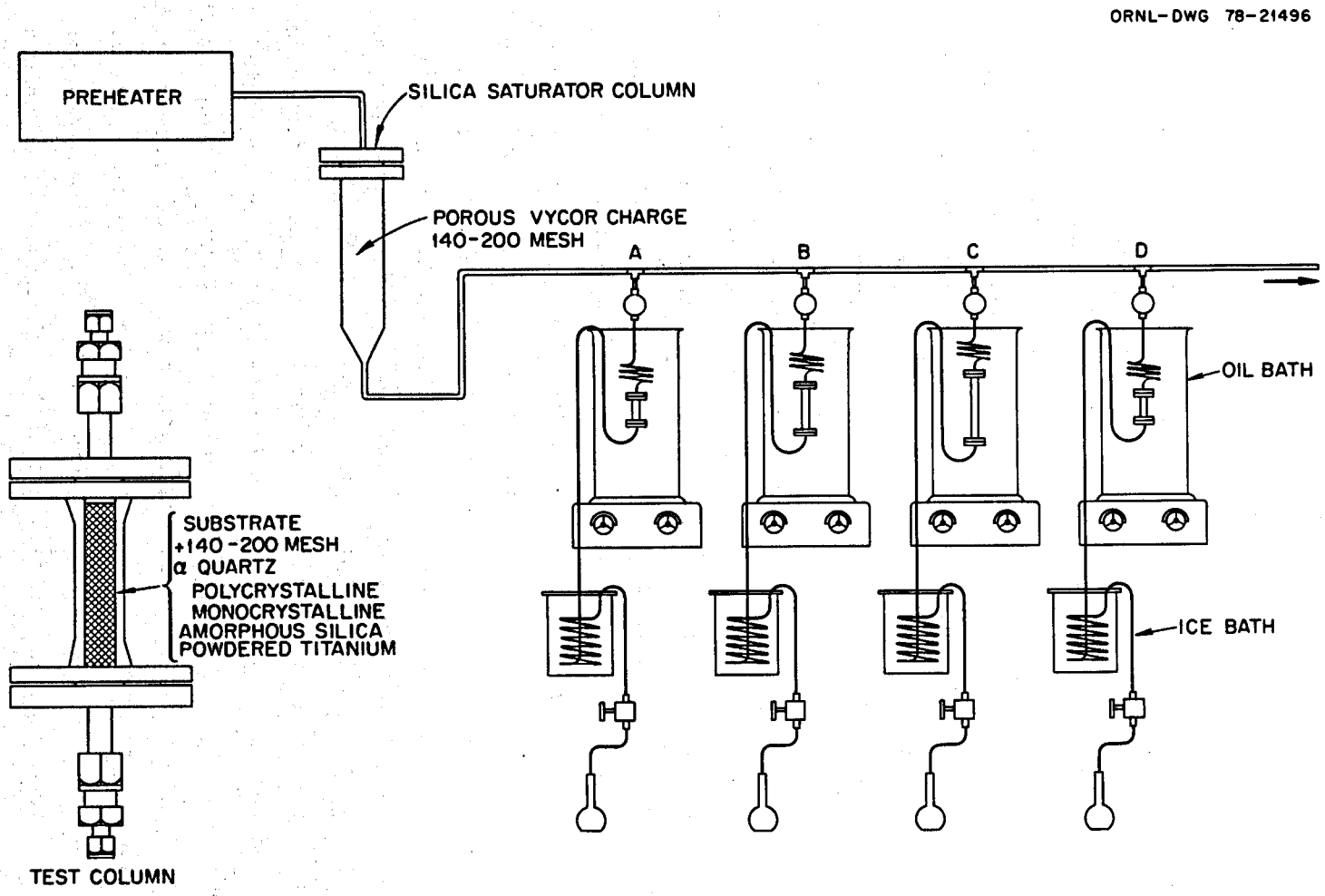


Fig. 1. Apparatus for studies of the kinetics of silica deposition on packed columns.

of homogeneous nucleation and polymerization in solution;

(2) The ease of sampling and quenching which are essential when the residence times are short (minutes); and

(3) The elimination of agitation and possible attrition caused by stirring as in a batch equilibration.

In addition, some exploratory column studies carried out previously clearly showed that the silica monomer deposits rapidly on an amorphous silica substrate (porous Vycor) but polymeric silica quite uniformly passed through the column unaffected. This is shown in Figs. 2 and 3 which are cross plots of the feed and effluent concentrations for solutions containing varying amounts of monomer and polymer in the range 100-1000 mg silica/kilogram of solution. With the monomer solutions the effluent concentration was always less than that of the feed, indicating deposition; whereas for the polymer solutions the data group around a 45° line indicating no interaction. These results gave pertinence to column studies in that they were consistent with field observations[22,23] which demonstrated as much as a thirty-fold reduction in silica deposition after waste brine ponding for a period long enough to substantially reduce the concentration of silica monomer by polymerization.

Two procedures were used to show that the column results were not influenced by simultaneous homogeneous polymerization of the silica. The first of these involved analysis of column effluent samples for total silica. Little or no polymeric material was found. As an additional check, the polymerization rates for various conditions were checked and the amount of polymerization was shown to be negligible for most conditions and retention times of interest. Thus as shown by the dashed curves in Fig. 4, the column reaction was 90% complete without significant polymerization having occurred in the same time period. These polymerization data were obtained by sampling column feed solution in a beaker in a constant temperature bath. The solid lines show a similar comparison under conditions favoring homogeneous polymerization - high pH, salinity, temperature, and with a low surface area substrate

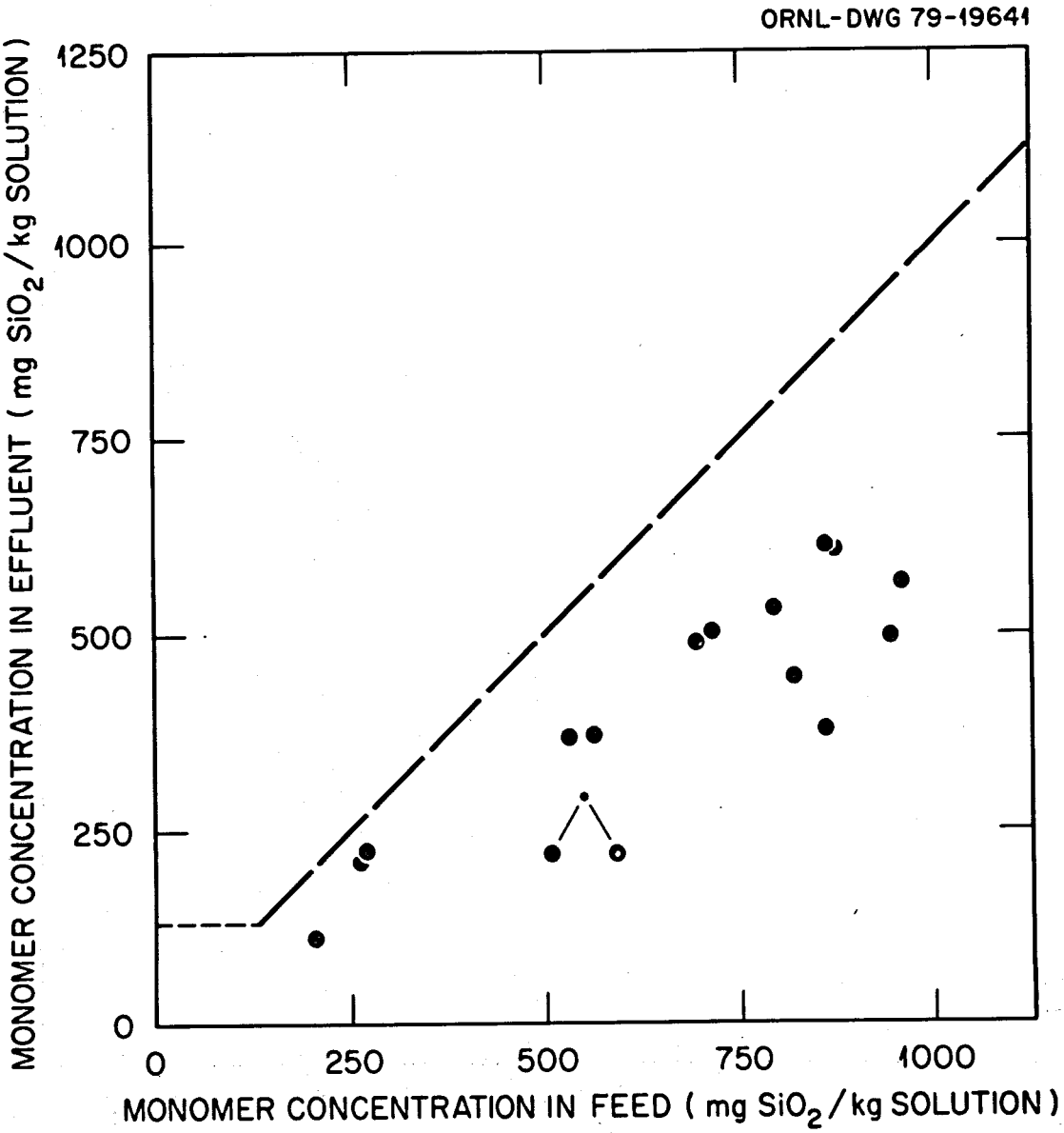


Fig. 2. Deposition of silica monomer on amorphous silica powder.

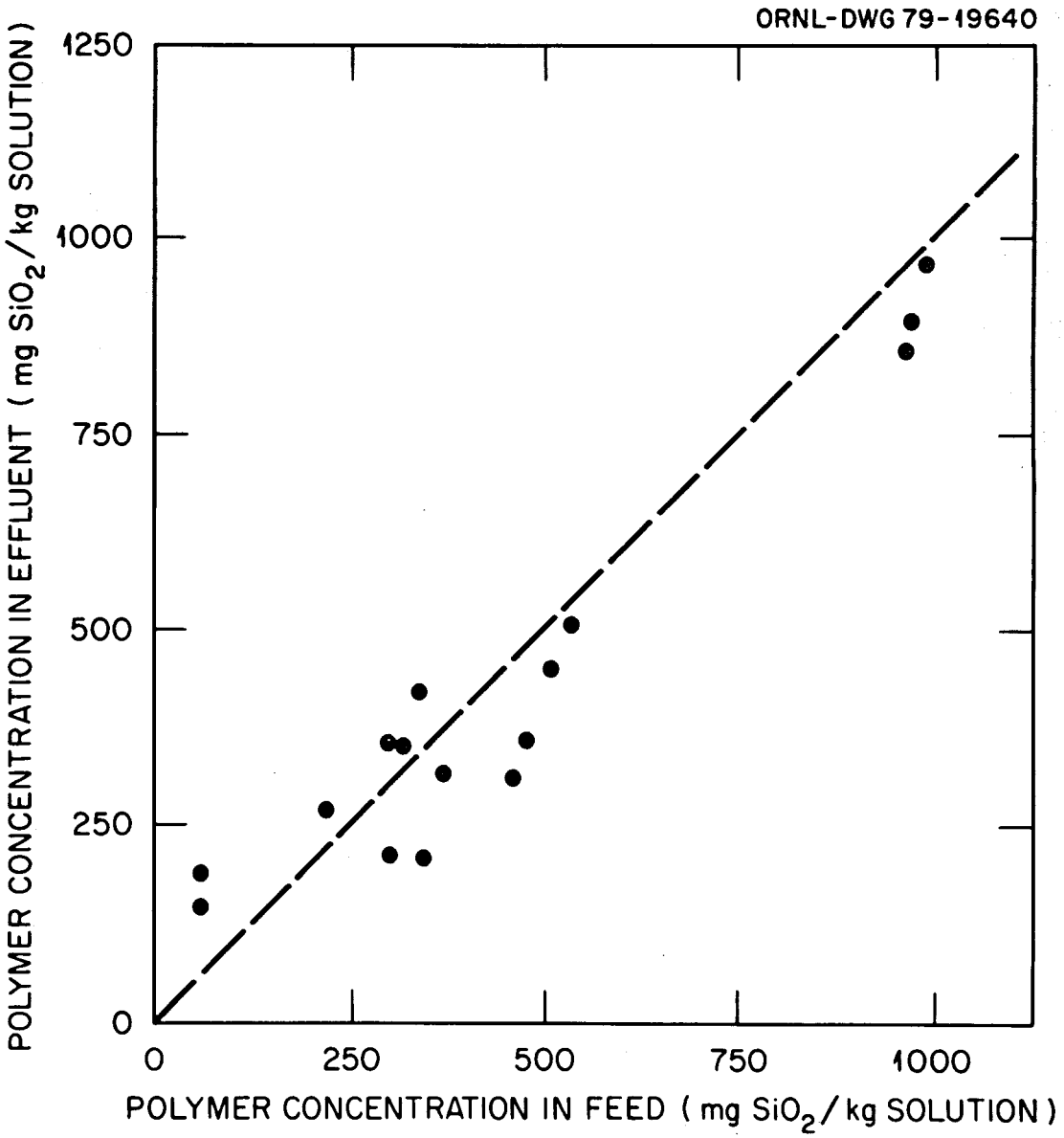


Fig. 3. Deposition of silica polymer on smorphous silica powder.

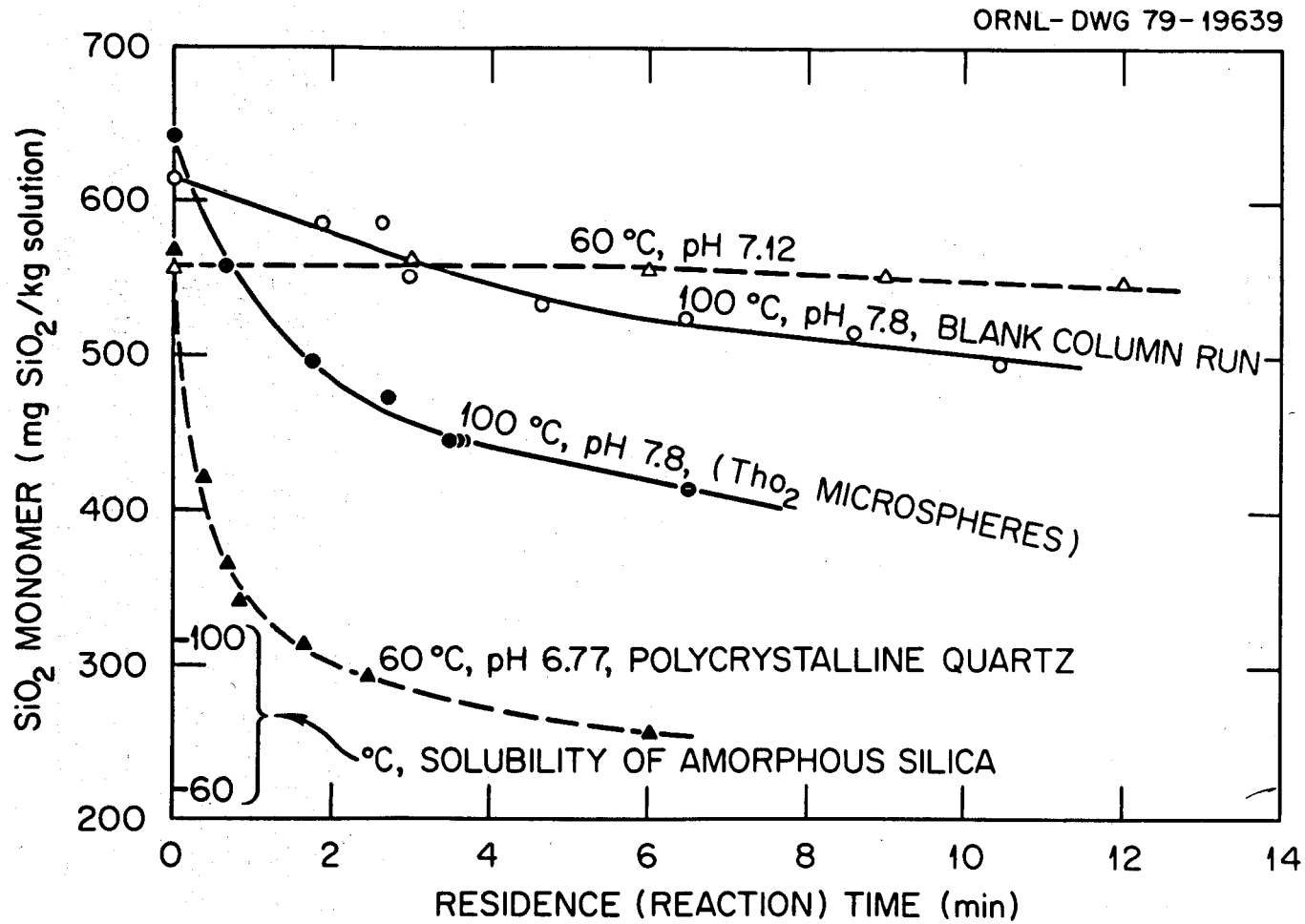


Fig. 4. Silica monomer deposition in packed columns (solid symbols) versus homogeneous polymerization in solution (open symbols) - 1 m NaCl, 0.1 m NaAc.

(coated $ThO_2$ microspheres). The polymerization data were obtained using an empty column setup and flow rates which gave retention times comparable to those of the packed column studies. Under these extreme conditions polymerization was appreciable in times of interest and could introduce appreciable error.

## 2.3 Substrates

Several substrates have been used in these studies, including:

Polycrystalline α quartz - aggregates of small angular grains individually less than 9 μm in diameter; aggregates average 70 μm and range to 350 μm. Fines were separated from the material used in the columns by Stokes column flotation with flow rates designed to remove particles smaller than 25-50 μm. Several percent of single crystal particles in the same size range (50-350 μm) were also present, as were small amounts of magnetic iron oxide particles.

A semiquantitative analysis of this material showed the following in addition to Si (in mg/kg): Al-400, Ca-20, Cr-5, Cu-10, Fe-1000, K-50, Mg-10, Mn-100, Na-30, P-25, U-5, Zn-5. The material was obtained from a mine in southern Illinois and was reported to be amorphous, but X-ray diffraction showed it was α quartz, as was also indicated by solubilities measured in attempting to use it as a charge for our saturator column. Some other characteristics for this, and the other substrates used in the kinetic studies, are given in Table 1.

Monocrystalline α quartz - single crystal material consisting of rounded grains ranging from 120 to 800 μm across. Under the microscope the material appeared appreciably cleaner and purer than the polycrystalline α quartz.

Porous Vycor - this is the same material as used in our saturator column. It was ground and sieved (-140, +200 mesh) and is amorphous silica containing about 3% $B_2O_3$ after leaching to give high porosity.

Powdered titanium metal powder - (-50, +100 mesh) and reported to be 99.7% Ti by the supplier.

Thoria microspheres - 210 to 240 μm spheres of very pure polycrystalline thorium oxide prepared by the sol-gel process.

Table 1. Some Characteristics of Substrates Used in Column Kinetic Studies

| Substrate | Morphology | Surface Area ($m^2/g$) | Void Vol. ($cm^3/g$) |
|---|---|---|---|
| Polycrystalline α quartz | Aggregates | 3.0 | 0.47 |
| Monocrystalline α quartz | Single crystal particles | 0.03 | 0.20 |
| Porous Vycor | Amorphous, porous particles | 164. | 0.70 |
| Powdered Ti metal | Aggregates and single particles | 2.4 | 0.48 |
| Thoria microspheres | Small spheres | 0.006 | 0.067 |

## 2.4 Column Preparation

Initial silica deposition on the columns is very much a function of the characteristics of the substrate, particularly the original surface area. Thus, the porous Vycor with very high (164 $m^2/g$) amorphous silica surface area quickly reduced the silica concentration in the column effluent to the equilibrium solubility at the temperature of operation; the materials with low area (0.03 $m^2/g$) monocrystalline α quartz and the thoria microspheres, on the other hand, removed very little silica during early column operation. The substrates with intermediate areas, polycrystalline α quartz and titanium powder, showed intermediate removal. Homogeneous polymerization during overnight shutdowns, when these occurred, may have played a part but did not affect the results.

During the first few tens of hours of column operation, the removal of silica by a column was quite erratic. After a time, however, depending on conditions, all substrates were "coated" with amorphous silica and gave quite reproducible results which were comparable for the

polycrystalline quartz, titanium metal powder and thoria microspheres. The effluent $SiO_2$ concentration during "coating" of a polycrystalline α quartz column is shown in Fig. 5. During the first three days of operation the results were erratic. However, after the substrate was fully coated with amorphous silica, reproducible results were obtained as a function of residence time. At that stage, as shown in Fig. 6, the relation between the silica removed by the column and residence time became quite reproducible. Thus, on 3/21 (X) the results still scattered considerably, but on 3/22 (O, Δ) the results check satisfactorily. The data at each of the three pHs are quite reproducible even though duplicate runs were carried out on different days or with different length columns.

2.5 Measurements and Calculations

The pH (negative logarithm of the hydrogen ion molality) measurements were based on standards containing 0.01 m HCl in 1.1 and 4.1 m NaCl and the hydroxide concentration was calculated using the known ion product of water in NaCl solutions.[24] Individual measurements are accurate to about 0.05 log units for the 1.1 m solutions and ∿ 0.1 log units for the 4.1 m.

Silica was determined by a procedure developed from that described by Grasshoff.[25] Three stock solutions were used:

(a) 2 M $(NH_4)_2SO_4$, pH 3.0

(b) 35.6 g $(NH_4)_6Mo_7O_{24}\cdot 4H_2O$ per liter

(c) 1.5 m $ClCH_2COOH$, pH 3 with $NH_4OH$

These solutions were mixed in the volume proportions 5:2:2 for a, b, and c and filtered. The mixture was added to 1 $cm^3$ of the unknown in a 50 $cm^3$ plastic volumetric flask and the color development measured at 390 nm after 10 minutes. The mixture could be used during an eight hour day but sometimes became hazy after standing overnight. The pH of the final mixture was kept between 3.0 and 3.2. The silica concentration was calculated from standards with 250 and 500 mg/kg $H_2O$ which were checked daily. In those samples where some polymerization had taken place, total silica was determined by digesting the 1 $cm^3$ sample aliquot with an equal volume of 30% NaOH for several hours or overnight, and

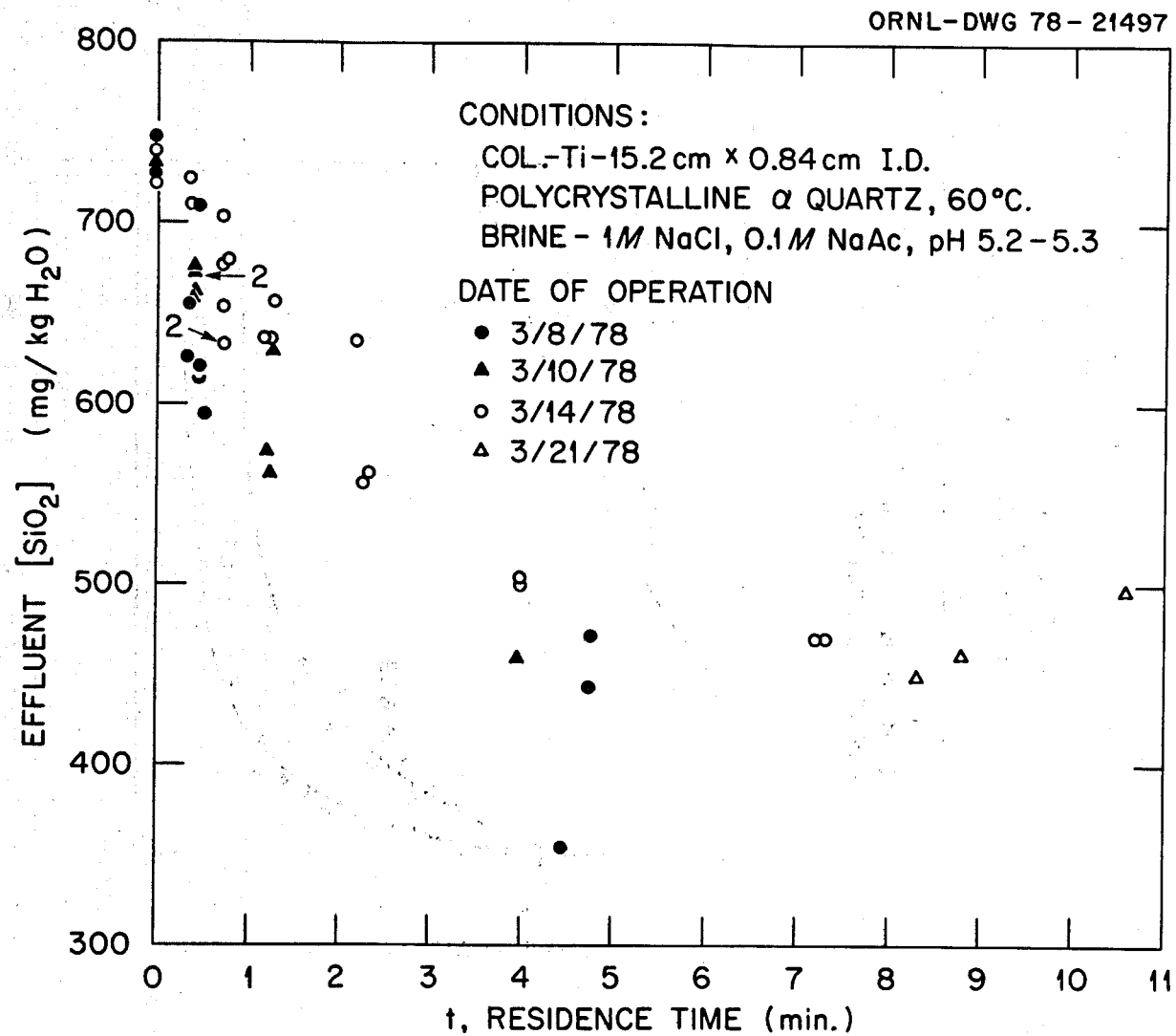


Fig. 5. Variable silica removal during column preparation.

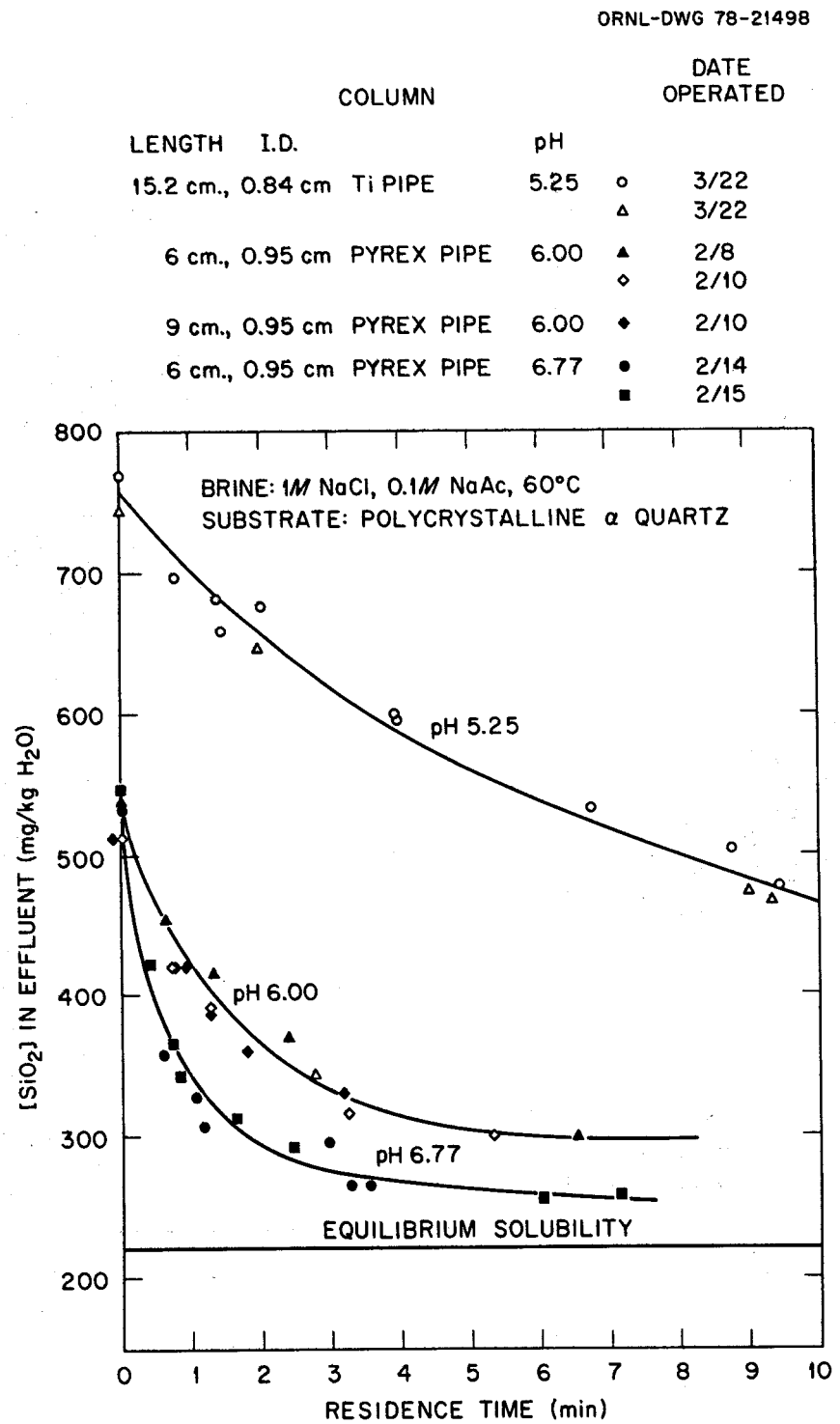


Fig. 6. Silica removal after column was "coated" with amorphous silica at 60°C in 1 m NaCl.

neutralizing the NaOH with 1 $cm^3$ of concentrated HCl (with the volumetric flask in an ice bath) just before adding the molybdate mixture. We estimate an overall analytical error of ±10 mg/kg $H_2O$ as $SiO_2$.

The residence time in the columns was established by dividing the column void volume by the measured flow rate in $cm^3$/min.

The weighting factors used in least squares analyses were obtained by assigning errors of (±10 mg/kg $H_2O$) to each silica determination in the term $(\underline{m} - \underline{m}_e)^{-1}$.

Surface areas were determined with a Digisorb 2500 Multigas Surface Area Analyzer.

## 3. RESULTS

### 3.1 Silica Concentration

Earlier studies of silica polymerization, wherein the molybdate reactive silica was followed and where the number of reactive sites of the polymerized silica was unknown, have found widely varying dependence on the silica concentration. The most often cited observation has been third order with respect to the supersaturation concentration, i.e., the concentration of monomeric silicic acid in the solution of interest minus the equilibrium solubility of amorphous silica in that solution; however, orders ranging from 0 to 3 have been reported by various investigators[9-17,26]. Thus, the determination of the reaction order for the deposition of silica from supersaturated brines was the first subject investigated.

First order dependence on supersaturation, $(\underline{m} - \underline{m}_e)$, is not indicated by the semi-log plots shown in Fig. 7. The values for $\underline{m}_e$ were taken from solubility measurements by Marshall[27] for amorphous silica in sodium nitrate solutions at these temperatures. Higher orders (2 and 3) were examined using the general equation described below. Data were fit with the integrated form of the following general rate expression (at constant pH)

$$-\frac{d\underline{m}}{dt} = k' \, (\underline{m} - \underline{m}_e)^n \qquad (4)$$

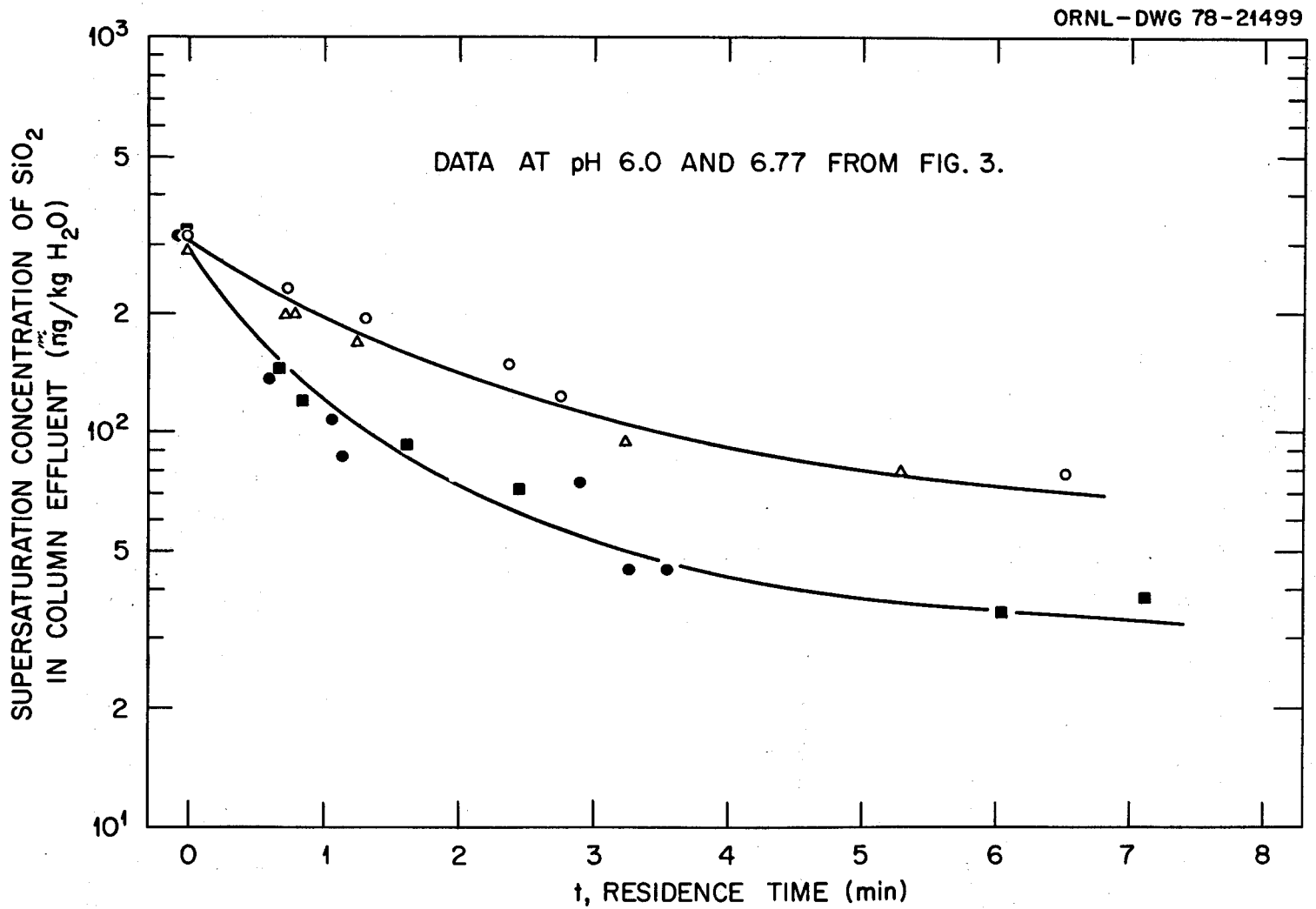


Fig. 7. Test of first-order dependence of silica deposition on coated polycrystalline quartz at 60°C in (1 m NaCl; 0.1 m NaAc) from Fig. 6.

which gives

$$\frac{1}{(m - m_e)^{n-1}} = \frac{1}{(m_o - m_e)^{(n-1)}} + (n-1)\, k'\, t \qquad (5)$$

where n is the order with respect to the supersaturation for n > 1, $\underline{m}$ is the molal concentration of dissolved silica [$Si(OH)_4$] in the column effluent, $\underline{m}_e$ is the equilibrium solubility of amorphous silica in the salt solution at temperature, and t is the residence time in the column. Second-order plots for three different pH values at 60°C are shown in Fig. 8. The agreement factors for a number of runs are tabulated in Table 2. While not uniquely so, the second order reaction is favored by these data. Data for most column studies carried out are summarized in Table 3. The apparent rate constants, k', were calculated using the second order rate law in terms of silica concentration. Dependence on the other parameters investigated is discussed below.

3.2 Hydroxide Concentration

The rapid acceleration of silica polymerization with increasing pH has been reported by a number of investigators[10,11,28,29]. Silica deposition has also shown similar behavior. From the data of Table 3 for polycrystalline quartz and several pH values the specific rate constant, k, was evaluated from the relationship

$$k' = kA\, [OH^-]^p \qquad (6)$$

where A is the BET surface area of the coated material in $cm^2$ per kg of water in the voids of the column bed. The variation of k' approaches an order of magnitude per pH unit and is consistent with the polymerization data of Makrides et al.[9,10] The hydroxide ion concentration used in the calculation of the specific rate constant in the last column of Table 3 was derived from the measured pH and the ion product of water in the brine at the temperature of the experiment. The exponent or order of the $[OH^-]$ term in the rate expression was obtained from a least squares fit of data obtained with two columns at pH values of 5.25, 6.00, and 6.76. Both the rate constant and the order for the hydroxide were

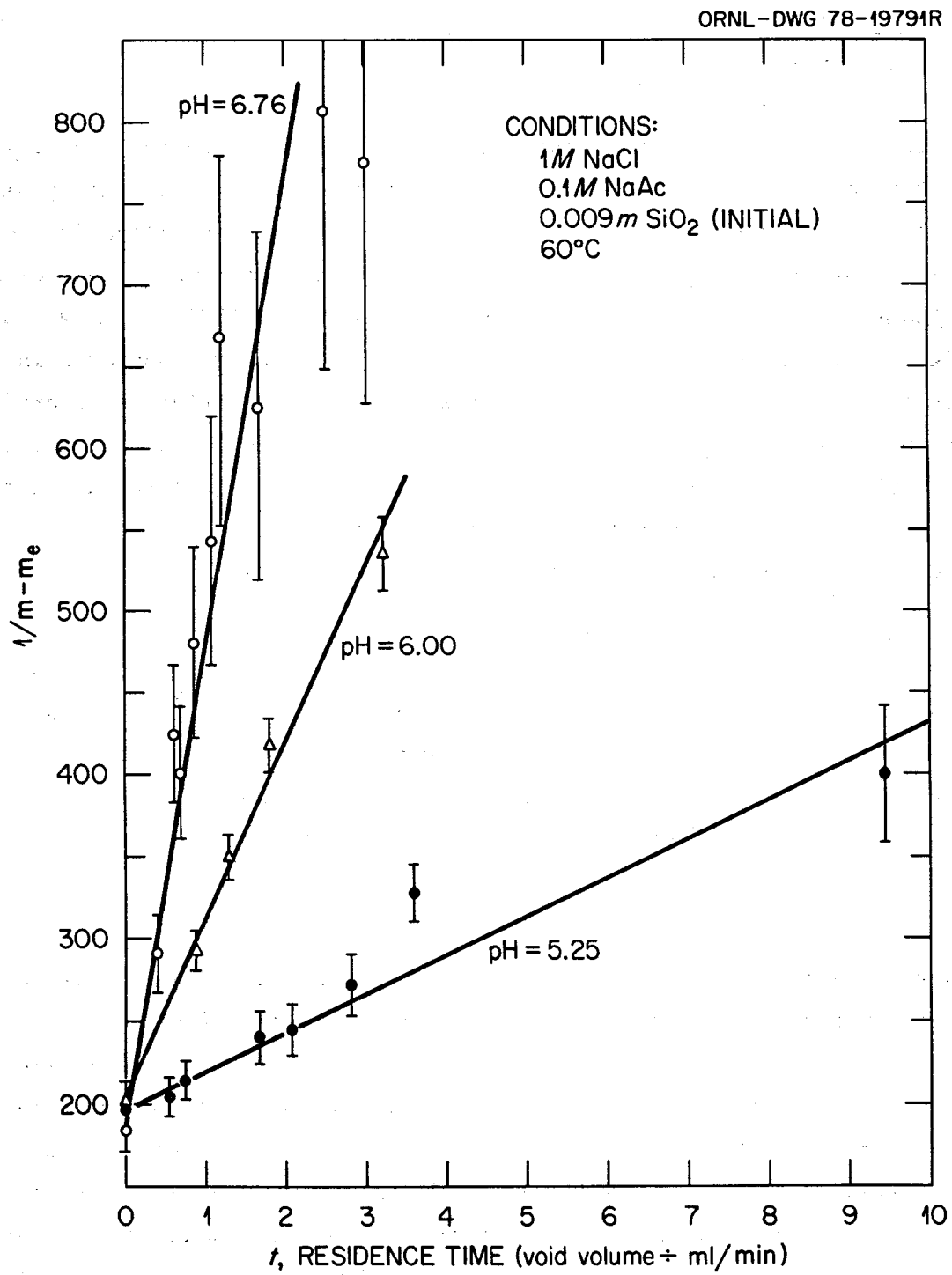


Fig. 8. Reciprocal supersaturation concentrations vs residence time as a function of brine pH. The linearity indicates second-order dependence on the supersaturation.

Table 2. Comparison of Least Square Fits for Second and Third Order Reactions

| Run No. | Column No. | Substrate | pH | Temp. °C | Agreement Factors 2nd Order (n = 2) | Agreement Factors 3rd Order (n = 3) |
|---|---|---|---|---|---|---|
| 10 OT | 1 | Polycryst. Qtz. | 6.02 | 60 | 0.951* | 1.038 |
| " | 1 | " | 6.76 | " | 0.919 | 0.901* |
| " | 1 | " | 5.25 | " | 0.975 | 0.903* |
| 12 OT | 1 | " | 5.25 | " | 1.382* | 1.487 |
| " | 1 | " | 5.32 | 80 | 0.732* | 1.161 |
| " | 1 | " | 5.35 | 100 | 0.290* | 0.893 |
| 12 OT | 2 | " | 5.33 | 100 | 0.512* | 0.957 |
| " | 1 | " | 5.35 | 60 | 0.561* | 0.636 |
| " | 4 | Ti Powder | 5.34 | 100 | 1.00 | 0.773* |
| 12 OT | 3 | Polycryst. Qtz. | 5.96 | 60 | 0.845* | 1.588 |
| " | 3 | " | 5.98 | 60 | 0.719* | 1.654 |

*The better fit of the two cases tested. The agreement factor is defined by

$$\sigma(y) = \left[\frac{\Sigma\, w_i (y_o - y_c)_i^2}{N_o - N_v}\right]^{1/2}$$

where $w_i$ is the weighting factor and $y_o - y_c$ is the difference in the observed and calculated values. $N_o$ is the number of observations and $N_v$ is the number of variables.

Table 3. Column Studies of Deposition of Silica From Brines

| Run | Column No. | pH | $[OH^-]^a$ mol/kg | $m_o$ $[SiO_2]$ mol/kg | $A^b$ $cm^2$/kg of $H_2O$ | Temp. °C | $k'^c$ kg/mol/min | $k^d$ |
|---|---|---|---|---|---|---|---|---|
| **Polycrystalline Quartz** | | | | | | | | |
| 7 | 1 | 6.07 | 2.24E-7 | .0085 | 2.22E-7 | 60 | 119. ± 7.8 | 0.24 |
| | 3 | 6.07 | 2.24E-7 | .0087 | 2.80E-7 | 60 | 195. ± 8.1 | 0.31 |
| 10 | 1 | 5.25 | 3.39E-8 | .0088 | 3.40E-7 | 60 | 28.5 ± 2.4 | 0.14 |
| | 2 | 6.00 | 1.91E-7 | .0088 | 4.69E-7 | 60 | 112. ± 3.7 | 0.12 |
| | 1 | 6.76 | 1.046E-6 | .0094 | 3.40E-7[e] | 60 | 300. ±19.1 | 0.14 |
| 12 | 1 | 5.35 | 4.27E-8 | .0127 | 0.64E-7 | 60 | 7.2 ± 0.2 | 0.16 |
| | 2 | 5.33 | 3.63E-7 | .0127 | 1.80E-7 | 100 | 94.1 ± 3.5 | 0.17 |
| | 3 | 5.98 | 1.82E-7 | .0127 | 0.79E-7 | 60 | 42.9 ± 1.0 | 0.28 |
| 13 | 1 | 6.00 | 1.91E-7 | .0090 | 0.95E-7 | 60 | 37.2 ± 2.5 | 0.15 |
| | 2 | 6.00 | 1.91E-7 | .0090 | 1.18E-7 | 60 | 21.1 ± 1.2 | 0.09 |
| **Porous Vycor** | | | | | | | | |
| 8 | 1 | 6.38 | 4.6E-7 | .0085 | 94.2E-7 | 60 | 51.9 ± 3.7 | 0.0015 |
| | 2 | 6.69 | 9.3E-7 | .0104 | 62.5E-7 | 60 | 46.5 ± 2.8 | 0.0012 |
| | 3 | 6.00 | 1.91E-7 | .0126 | 54.9E-7 | 60 | 6.44± 0.28 | 0.0006 |
| **Monocrystalline Quartz** | | | | | | | | |
| 10 | 3 | 6.77 | 1.12E-6 | .0096 | 0.11E-7 | 60 | 35.1 ± 2.0 | 0.47 |
| | 4 | 6.00 | 1.91E-7 | .0088 | 0.074E-7 | 60 | 15.6 ± 0.84 | 1.06 |
| **Titanium Powder** | | | | | | | | |
| 12 | 4 | 5.34 | 3.72E-7 | .0127 | 1.11E-7 | 100 | 40.4 ± 2.8 | 0.11 |
| 13 | 4 | 6.00 | 1.91E-7 | .0090 | 8.19E-6 | 60 | 18.9 ± 1.42 | 0.12 |
| **Thoria Microspheres** | | | | | | | | |
| 13 | 3 | 6.00 | 1.91E-7 | .0090 | 5.68E-5 | 60 | 2.21± 0.47 | 0.10 |

[a] $[OH^-]$ calculated from pH measurement and $Q_w$.

[b] $cm^2$ per kg of water in void volume.

[c] Apparent rate constant - area and $[OH^-]$ included.

[d] Specific rate constant (units omitted because of fractional power of hydroxide concentration).

[e] This column was subsequently run at pH 5.25, but so little $SiO_2$ was added it was deemed appropriate to use the final area for this run too.

allowed to vary in obtaining the value of 0.70 ± 0.16 for p.

### 3.3 Surface Area

The surface area of the substrate is, of course, a significant factor in the reaction rate. The area to be considered, however, is that which was present after the original substrate was coated as described previously. We have used the BET surface areas determined by nitrogen or krypton adsorption after drying the column material at 125°C under vacuum. It was determined by experiment that the area was independent of the drying temperature from 25° to 500°C. Note that the differences in density of substrates do not enter the rate considerations since the total area of the column is used.

The results for polycrystalline quartz, titanium powder and initially thoria microspheres were remarkably consistent when the surface area was taken into account. The rate constants computed for porous Vycor were much too low compared to these materials and suggest that large amounts of the internal area is unavailable for silica deposition. We have no ready explanation for the somewhat higher rate constants shown in Table 3 for the monocrystalline quartz.

During the temperature studies (see below), which used $ThO_2$ microspheres as the initial substrate, it became evident that the surface areas of the coated spheres were below the range for measurement with the techniques used. However, scanning electron microscope examination of the coated spheres showed the coating approximated covering the original surface with many small hemispheres (Fig. 9) which would double the original area. The original microspheres (225 ± 15 μm dia) had a calculated area of 27 $cm^2/g$, so 50 $cm^2/g$ was chosen for the coated area. A calibration run in 1 m NaCl at 60°C produced a specific rate constant of 0.13 in agreement with previous data for those conditions, thereby giving support for the choice. BET areas which were measured also scattered randomly about the 50 $cm^2/g$ value.

An interesting sidelight was a run conducted with coated $ThO_2$ which had been dried at 125°C under vacuum and carried through the surface area analysis procedure. A k value of 0.18 was obtained for this material in spite of this treatment and with no prior re-conditioning.

PHOTO 5048-79

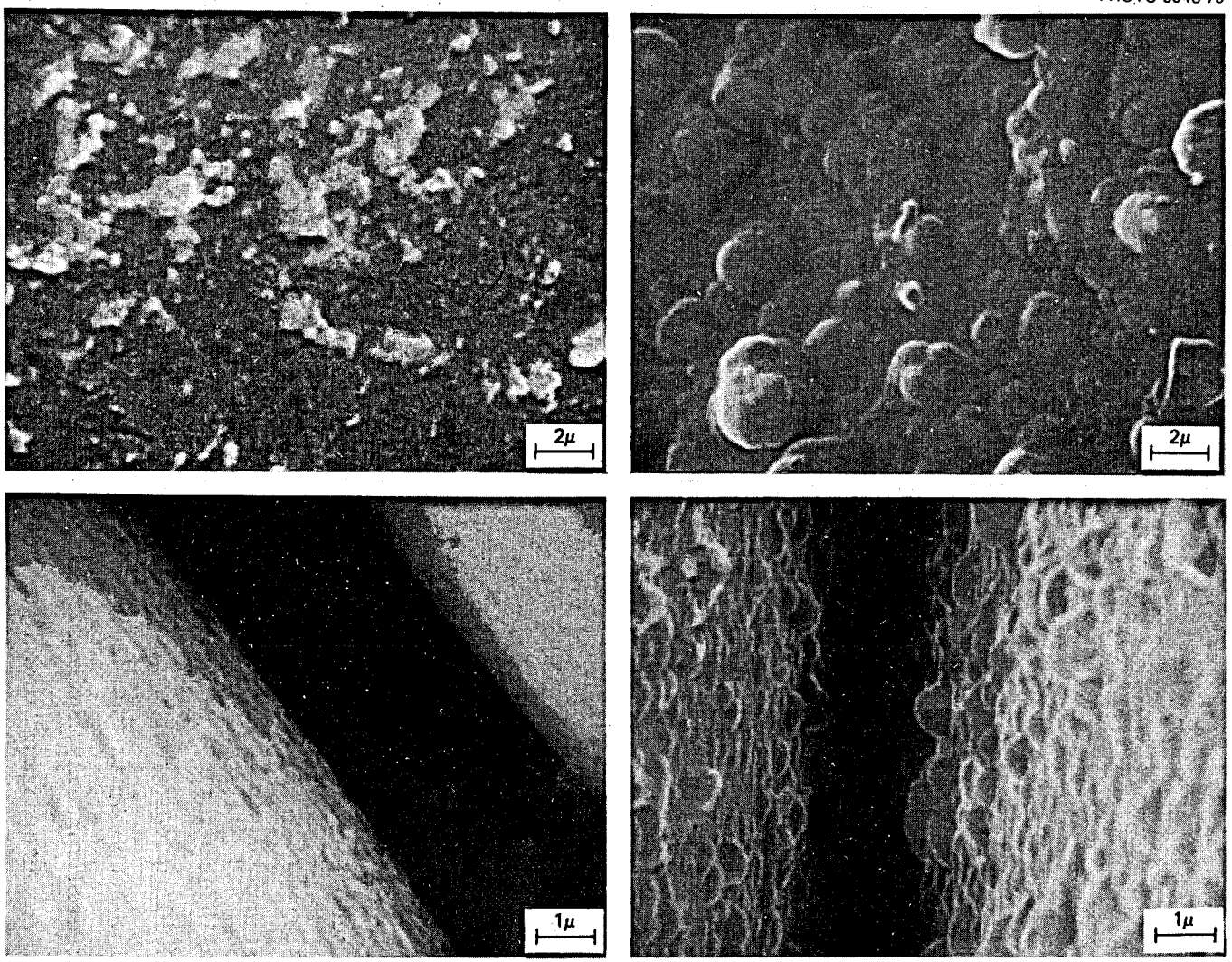


ORIGINAL $ThO_2$ MICROSPHERES

AFTER COATING WITH AMORPHOUS SILICA

Fig. 9. Thoria microspheres before and after coating with amorphous silica.

### 3.4 Temperature

The data in Table 4 show no effect of temperature (60° to 100°C) when resultant changes in hydroxide ion concentration are taken into account. However, it was noted that when the temperature was changed it took several hours of operation to "condition" the column before the second order dependence on silica concentration was again observed.

A second series was run which gave similar results. Initial column operation at the higher temperature gave scattered results; however, subsequent operations resulted in reasonable second order dependence on silica supersaturation. The rate constants calculated as for the previous studies with corrections for temperature effects on the ionization constant for water are consistent with those obtained previously. Within our limits of error, no temperature effect is indicated (at constant hydroxide concentration). However, the polymerization reaction has been reported[10] to show little or no dependence on temperature at constant pH. The necessity for reconditioning the column suggests the detailed deposition mechanism is changing with temperature. On one occasion a column which had been run at increasing temperatures 60→80→100°C was subsequently run again at 60°C. The second order silica concentration dependence was maintained and the rate constant fell within the range of previous values obtained at 60°C (0.16).

### 3.5 Sodium Chloride Concentration

Results of a brief survey of the effect of sodium chloride concentration are summarized in Table 5. The runs were made with the coated polycrystalline quartz so that surface areas could be precisely measured. Decreasing the salt concentration to 0.086 m reduces the rate by only a factor of two compared to 1 m, but raising the salt concentration to 4 m increased the rate by a factor of 20. Another run at 4 m with the coated thoria microspheres gave a value of 6.2 for the rate constant but a subsequent run at 1 m NaCl suggested the area in this case may have been sufficiently higher than the assumed 50 $cm^2/g$. Time did not permit further investigations of salinity and temperature effects as the program had been terminated as of the end of FY 1978.

Table 4. Effect of Temperature on Second Order Rate Constant for Silica Deposition from 1 m NaCl, 0.1 m NaAc, 0.01 m $NaHCO_3$; $ThO_2$ Microsphere Substrate

| Temperature | pH | | k' | Area/kg $H_2O$ in Voids | $[OH^-]^{0.7}$ | k |
|---|---|---|---|---|---|---|
| (°C) | HCl std.[a] | 23°C, NBS | kg/mol/min | $cm^2$[b] | | |
| 60 | 7.85 | 8.04 | 50.8 | 7.47E + 5 | 5.21E − 4 | 0.13 |
| 80 | 7.65 | 7.87 | 62.1 | 7.47E + 5 | 6.73E − 4 | 0.095 |
| 100 | 7.70 | 7.94 | 69.4 | 7.47E + 5 | 1.89E − 3 | 0.049 |
| 120 | 7.71 | 7.96 | 80.8 | 7.47E + 5 | 2.08E − 3 | 0.031 |

[a] Using 1.1 m NaCl + 0.02 m HCl as reference.

[b] 50 $cm^2/g$, see text.

Table 5. Effect of Sodium Chloride Concentration on Specific Rate Constant for Silica Deposition at 60°C

| [NaCl] m | [NaAc] m | $(F^-)$ mg/kg | pH | | k' kg/mol/min | Area/kg $H_2O$ in Voids ($cm^2$/kg) | $[OH^-]^{0.7}$ | k |
|---|---|---|---|---|---|---|---|---|
| | | | HCl std.[a] | 23°C, NBS | | | | |
| 0.086 | 0.1 | — | 6.00 | 5.98 | 48.3 | 3.25 E + 7 | 1.80E − 5 | 0.083 |
| 0.086 | 0.1 | — | 5.92 | 5.90 | 43.5 | 4.05 E + 7 | 1.58E − 5 | 0.067 |
| 0.086 | 0.1 | 25 | 5.94 | 5.92 | 46.6 | 4.05 E + 7 | 1.63E − 5 | 0.071 |
| 1.0 | 0.1 | — | 6.00 | 5.98 | 112 | 4.69E + 7 | 5.51E − 5 | 0.12 |
| 4.0 | 0.1 | — | 4.70 | 6.05 | 86 | 3.25E + 7 | 1.08E − 6 | 2.45 |

[a] pH at temperature with 0.01 m HCl in the presence of the medium salt as the reference.

### 3.6 Fluoride Ion Catalysis

Makrides et al.[10] observed substantial increases in silica polymerization rates with the addition of small amounts of (20 to 100 mg/kg) fluoride ion at pH 4.5. At the end of the low salinity runs (pH 5.94), 25 mg/kg of fluoride ion was added to the brine but no change in the deposition rate was observed - see Table 5. Similar negative results were reported by Weres et al.[30] above pH 5.

## 4. EMPIRICAL RATE EQUATION

The empirical rate equation which describes our data in 1 m NaCl in the pH range 5-8 and temperatures from 60-120°C is

$$-\frac{d[Si(OH)_4]}{dt} = 0.12A\,([Si(OH)_4] - [Si(OH)_4]_{eq})^2\,[OH^-]^{0.7} \qquad (7)$$

where A is the surface area in $cm^2$ $SiO_2$ per kg of water in column voids, t is in minutes, and the concentrations are in molal units. Hydroxide concentration was derived from the measured pH and the ionization quotient for water. In the expression given above the rate constant is essentially independent of temperature over the range 60-120°C. Alternatively the rate of linear growth of an amorphous silica surface in cm/min is given by

$$\frac{dh}{dt} = 3.1\,([Si(OH)_4] - [Si(OH)_4]_{eq})^2\,[OH^-]^{0.7} \qquad (8)$$

The effect of salinity on the rate was not included because of the limited data and the apparent complexity of the dependence.

## 5. DISCUSSION

Many investigators have found that the polymerization of silica from supersaturated brines is substantially enhanced as the supersaturation, pH, and salinity are increased. The same parameters might be expected to have importance in the deposition of amorphous silica

scales from supersaturated brines. Additional constituents which have been discussed are fluoride,[10] sulfides,[31] and other mineral species found in silica scales.[32] Our studies, consistent with other observations, have shown that hydrodynamics also plays a significant role, e.g., valves are more prone to scale than pipe runs.[28]

Early concerns of these column studies addressed the questions:

Which species are involved in the deposition reaction?

Is the process under diffusion or interface reaction control?

## 5.1 Identity of the Depositing Species

The first of these questions was addressed by conducting the experiments described above in which only monomeric silicic acid (rapid molybdate reaction species) was present in the input solution under conditions where no significant polymerization occurred during the residence time on the column. We found that under various conditions more than half of the silica was deposited directly from the monomer solution. In other experiments we examined the relative deposition of monomeric silica and polymerized silica from the same solution (see Figs. 2 and 3). Again, the monomeric species was shown to be depositing while there was little or no tendency for deposition of the previously polymerized silica. Interestingly, the deposited material often occurs as interlaced spheroids which are well cemented by a fine matrix as shown in Fig. 10.[32]

## 5.2 Deposition Rate Control

There are three kinds of evidence that the deposition process is not diffusion (in the liquid phase) controlled: (1) the slow equilibration rate in a packed bed, (2) the independence of silica deposition on flow rate in a packed bed, and (3) the dependence of the rate on hydroxide concentration.

In applying the first of these criteria the equilibration time expected in a stationary liquid phase in a packed column was estimated using the method of Kraus et al.[33]

$$\tau < (R^2/D)\ [-0.05 - 0.233 \log \Delta] \ . \qquad (9)$$

Y-144515

Silica Scale Formed on Pyrex Pipe in Once-Through System
Run No. 1
Conditions: 0.1 M NaAc, 1 M NaCl, pH 6, 725 ppm, $SiO_2$ (seedec

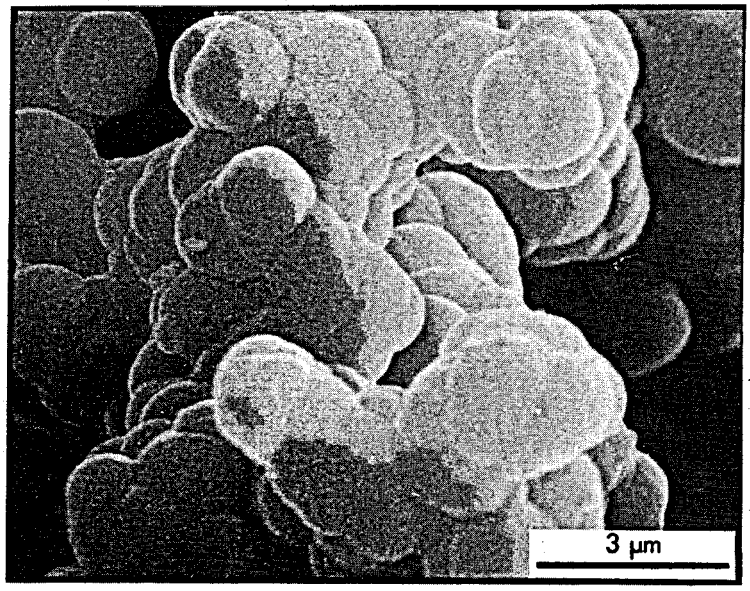


Deposition Temperature, 146°C - 10,000X

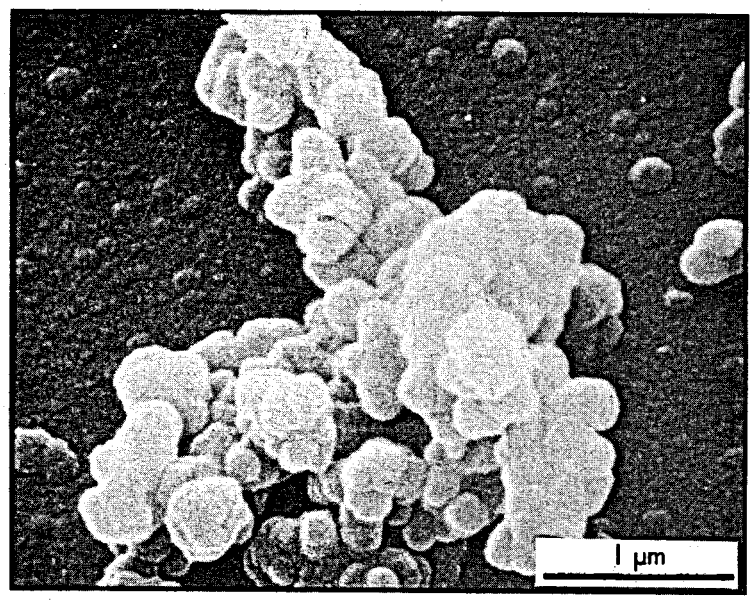


Deposition Temperature, 56°C - 28,000X

Fig. 10. Spheroidal cluster morphology of amorphous silica deposits from supersaturated brine.

Assuming $R \sim 0.005$ cm, $D \sim 10^{-5}$ $cm^2/sec$ and $\Delta$ (the complement of the fractional attainment of equilibrium, e.g., 0.01 for 99% of equilibria), the value of $\tau$ is less than 1 sec for $\Delta$ of 0.01 or 0.05 sec for $\Delta$ of 0.5. Of course, in a flowing system one would expect lower equilibration times than estimated by equation (9) because of the thinner diffusion layer. In all our experiments equilibration times were much greater ($> 10^4$ times) than the values estimated above.

In a flowing system the diffusion film thickness is related to the flow rate, yet we observed no dependence of the equilibration time or silica removal on flow rate when the residence time was kept constant by changing the column length.

The dependence of the kinetics on hydroxide concentration, to be discussed later, also shows that the process is reaction limited.

5.3 Mechanism of Deposition

Although it has been demonstrated by this work that monomeric silica will deposit directly without previous polymerization, little mechanistic detail can be deduced from the observed crystal-growth kinetics showing greater than first-order dependence on the supersaturation concentration. Since our data were best fit with an order of $0.7 \pm 0.16$ for the hydroxide concentration, the predominant process can reasonably be thought of as hydroxide catalyzed. In the case where $\underline{m}$ approaches $\underline{m}_e$, the observed kinetics is consistent with the following simple processes:

$$Si(OH)_4(aq) + OH^- \rightleftarrows Si(OH)_3^- + H_2O \qquad (10)$$

$$Si(OH)_4(aq) + SiO(OH)_3^- \rightleftarrows SiO_2(am) + 3H_2O + OH^- \qquad (11)$$

where the first is the simple ionization equilibrium and the second is a bimolecular step in which the catalyst, hydroxide ion, is regenerated. This process leads to a rate law of the form

$$-\frac{d\underline{m}}{dt} = k(\underline{m}^2 - \underline{m}_e^2)\,[OH] \qquad (12)$$

which approaches the observed dependence on supersaturation as $m$ approaches $m_e$.

The pH or hydroxide dependence suggests the participation of the silicate species as was also suggested by Makrides et al.[10] for the polymerization studies.

## 5.4 Applications

With equations (7-8) one can estimate silica deposition rates on previously coated surfaces. Figure 11 illustrates that a maximum rate is observed at constant pH (6) as the temperature increases; this results from the opposing effects of rapid increase in hydroxide concentration (from the changing ion product for water) and the decreasing supersaturation. The position of the maximum also increases sharply and shifts toward higher temperatures as the silica concentration increases. The model represents the condition where short residence times are considered and homogeneous nucleation is not a competing process. By incorporation of the model for homogeneous nucleation and kinetic behavior at the early stages of polymerization presented by Makrides et al.,[10] one could possibly model more complex real systems. However, many details such as heterogeneous nucleation behavior, and the specific effects of partially covered substrates and hydrodynamics on growth rates are not known. The rate of change of specific area of the coated deposit with deposition and the relationship between the surface area of the deposit and the surface area of the substrate are also unknown at this time.

With the possibility of prolonged contact with natural silicates and silica, one would predict rapid plugging of underground formations; a principal concern regarding the reinjection of waste geothermal brines. From the kinetics reported here we calculate that the linear growth rate of a surface at pH of 7 at 100°C and supersaturation of 0.006 (360 mg/kg) is 0.6 μm per day. Such rates will reduce porosity in the vicinity of the reinjection and likely lead to plugging in short times. This result is consistent with the recent field experience.[34]

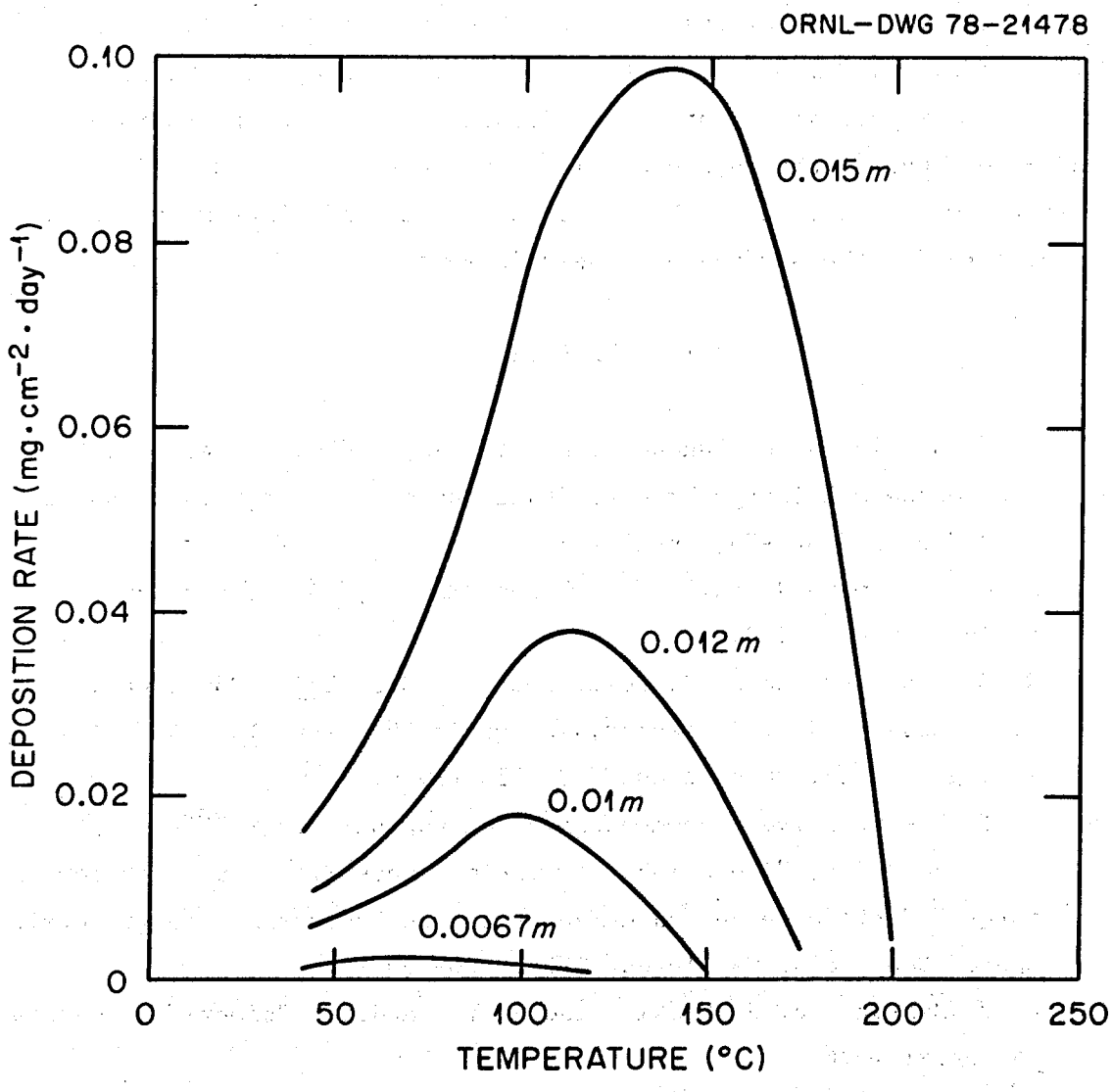


Fig. 11. Calculated rate of deposition of amorphous silica vs temperature and silica concentration at pH 6 in 1 m NaCl.

ACKNOWLEDGMENTS

The authors wish to acknowledge the helpful discussions with the following colleagues of the Chemistry Division at ORNL: A. J. Shor, F. A. Posey, F. Nelson, C. F. Baes, Jr., R. H. Busey, and W. L. Marshall. We are also grateful to Frances L. Ball, R. L. Sherman, and H. W. Dunn of the Physicochemical Analysis Group at ORNL for electron microscopy and to L. L. Jones of the Y-12 plant Micromeritics Laboratory for the surface area measurements.

REFERENCES

1. A. L. Austin, A. W. Lundberg, L. B. Owen, and G. E. Tardiff, "The LLL Geothermal Energy Program Status Report, January 1976-January 1977," UCRL-50046-76, April 1977.
2. H. C. H. Armstead (ed.), "Geothermal Energy," The Unesco Press, Paris, France, 1973.
3. R. O. Fournier and J. J. Rowe, Amer. J. Sci. 264, 685 (1966).
4. R. H. Busey and R. E. Mesmer, Inorganic Chemistry 16, 2444 (1977).
5. N. Ingri, Acta. Chem. Scand. 13, 758 (1959).
6. R. H. Busey, private communication on unpublished work.
7. R. O. Fournier, "The Solubility of Amorphous Silica at High Temperatures," Conference on Scale Management in Geothermal Energy Development," San Diego, CA, August 1976, COO-2607-4.
8. R. J. Darragh, A. J. Gaskin, and J. V. Sanders, Scientific American 84, April 1976.
9. W. W. Harvey, M. J. Turner, J. Slaughter, A. C. Makrides, EIC Corp., 55 Chapel Street, Newton, MA 02158, "Study of Silica Scaling From Geothermal Brines," Progress Report for Period March 1976-September 1976, COO-2607-3 (October 1976).
10. A. C. Makrides, M. J. Turner, W. W. Harvey, J. Slaughter, S. B. Brummer, P. O'D. Offenhartz, G. F. Pearson, EIC Corp., 55 Chapel Street, Newton, MA 02158, "Study of Silica Scaling From Geothermal Brines," Final Report, COO-2607-5, January 1978.

11. M. Cordurier, B. Baudru, J. B. Donnet, Bull. Soc. Chim., France 3147, 3154, 3161 (1971).
12. H. P. Rothbaum and R. D. Wilson in "Geochemistry 1977," New Zealand, Department of Sci. and Ind. Res. Bull. 218, p. 37, Wellington, 1977.
13. A. D. Bishop and J. L. Bear, Thermochimica Acta 3, 399 (1972).
14. S. Kitahara, Rev. Phys. Chem., Japan 30, 131 (1960).
15. T. Jarutani, J. of Chromatography 50, 523-6, 1970.
16. H. Baumann, Koll. Zeit. 162, 28 (1959); Z. Anal. Chem. 217, 241 (1966).
17. G. B. Alexander, J. Am. Chem. Soc. 76, 2094 (1954).
18. D. Elwell and H. J. Schell, "Crystal Growth from High-Temperature Solutions," Academic Press, New York (1975).
19. G. H. Nancollas and N. Purdie, Quarterly Reviews.
20. R. A. Laudise, "The Growth of Single Crystal," Prentice-Hall, Inc., Englewood Cliffs, New Jersey (1970).
21. R. H. Doremus, J. Phys. Chem. 62, 1068 (1958).
22. G. Cuellar, "Behavior of Silica in Geothermal Waste Water," Proceedings, Second UN Symposium on the Development and Use of Geothermal Resources, May 20-29, 1975, Vol. 2, pp. 1337-1347.
23. H. P. Rothbaum, private communication (submitted for publication in Geothermics, 1979).
24. R. H. Busey and R. E. Mesmer, J. Chem. Engr. Data 23, 175 (1978).
25. K. Grasshoff, Deep Sea Research 11, 597-604, 1964.
26. A. R. Marsh, G. Klein, and T. Vermeulen, "Polymerization Kinetics and Equilibria of Silicic Acid in Aqueous Systems," LBL 4415, Oct. 1975.
27. W. L. Marshall, unpublished data by private communication.
28. E. G. Bohlmann, A. J. Shor, and P. Berlinski, "Precipitation and Scaling in Dynamic Geothermal Systems," ORNL/TM-5649, Oct. 1976.
29. K. Goto, Geochim. Cosmochim. Acta 12, 123 (1957).
30. O. Weres, A. Yee, L. Tsao, Proceedings, Society of Petroleum Engineers International Symposium on Oilfield and Geothermal Chemistry, Houston, TX, Jan. 22-24, 1979, p. 249.
31. B. J. Skinner, D. E. White, H. J. Rose, and R. E. Mays, Econ. Geol. 62, 316-330+ (1967).

32. E. G. Bohlmann, A. J. Shor, and P. Berlinski, "Precipitation and Scaling in Dynamic Geothermal Systems," ORNL/TM-5959, July 1977.

33. L. B. Owen, "Precipitation of Amorphous Silica from High-Temperature Hypersaline Geothermal Brines," UCRL-51866, June 1975.

34. K. A. Kraus, H. O. Phillips, and F. Nelson, Proceedings of the IAEA Conference, Copenhagen, September 1960, on "Radioisotopes in the Physical Sciences and Industry," Vol. III, 387 (1962).

35. R. H. Messer, D. S. Pye, and J. P. Gallus, J. of Petroleum Technology (Sept. 1978), 1225-1230.

ORNL/TM-7117
UC-4 Chemistry

INTERNAL DISTRIBUTION

1-2. Central Research Library
3. ORNL Patent Office
4. ORNL-Y-12 Technical Library, Document Reference Department
5. Laboratory Records, ORNL, RC
6-7. Laboratory Records Department
8. C. F. Baes, Jr.
9. F. Ball
10. P. Berlinski
11-15. E. G. Bohlmann
16. R. H. Busey
17. J. DeVan
18. F. W. Dickson
19. E. L. Fuller
20. J. Griess
21. H. Hoffman
22. H. F. Holmes
23. J. S. Johnson
24. O. L. Keller
25. W. L. Marshall
26-30. R. E. Mesmer
31. J. Michel
32. M. T. Naney
33. F. A. Posey
34. A. J. Shor
35. R. A. Strehlow
36. D. Thomas
37. I. L. Thomas

EXTERNAL DISTRIBUTION

38. J. F. Addoms, Aeroject Liquid Rocket Co., PO Box 13222, Dept. 9732, Sacramento, CA 95670
39. D. N. Anderson, State of California, 1111 Howell Ave., Sacramento, CA 95825
40. J. A. Apps, Energy and Environment Div., Lawrence Berkeley Laboratory, Berkeley, CA 94720
41. S. Arnorsson, National Energy Authority, Laugavegur 116, Reykjavik, ICELAND
42. R. C. Axtmann, Princeton University, School of Engineering/Applied Science, Dept. of Chemical Engineering, The Engineering Quadrangle, Princeton, NJ 08540
43. J. Balagna, LASL, Los Alamos, NM 87545
44. H. L. Barnes, Pennsylvania State University, 208 Deike Building. University Park, PA 16802

45. H. Bishop, San Diego Gas and Electric, PO Box 1831, San Diego, CA 92112
46. B. Breindel, Aerojet Energy Conversion, PO Box 13222, Sacramento, CA 95813
47. R. W. Charles, Los Alamos Scientific Laboratory, CNC-11, MS 514, Los Alamos, NM 87545
48. G. L. Chierici, AGIP S5A, PO Box 4174, Milano, ITALY I-20100
49. A. G. Collins, DOE, PO Box 1398, Bartlesville, OK 74003
50. G. Crane, Southern California Edison, PO Box 800, Rosemead, CA 91770
51. W. F. Downs, EG8G Idaho, Inc., PO Box 1625, Idaho Falls, ID 83401
52. W. A. Edmiston, Jet Propulsion Laboratory, California Institute of Technology, Pasadena, CA 91103
53. A. J. Ellis, Chemistry Div., Dept. of Scientific and Industrial Research, Private Bag, Petone, NEW ZEALAND
54. H. E. Englander, Chevron Oil Field Research Laboratory, PO Box 446, La Habra, CA 90631
55. R. P. Epple, DOE, Washington, DC 20545
56. R. C. Feber, Los Alamos Scientific Laboratory, PO Box 1663, Los Alamos, NM 87545
57. O. W. Flörke, Institut fur Mineralogie, Ruhr-Universitat Bochum, D-4630 Bochum, WEST GERMANY
58. R. O. Fournier, U. S. Geological Survey, Stop 18, 345 Middlefield Road, Menlo Park, CA 94025
59. D. L. Gibbon, Calgon Corp., Box 1346, Pittsburgh, PA 15230
60. A. E. Gorum, Oximetrix, 1215 A Terra Bella Ave., Mountainview, CA 94043
61. J. Guiza, Federal Commission of Electricity, Melchor Ocampo No. 455-4° piso, MEXICO 5, D. F.
62. G. Hajela, Atomics International, 8900 DeSoto Ave., Canoga Park, CA 91304
63. B. A. Hall, Geothermal Resources Council, PO Box 1033, Davis, CA 95616
64. H. Harris, Monsanto Co., 800 N. Lindbergh Blvd., Mail Zone N-3D, St. Louis, MO 63166
65. J. A. Heist, Concentration Specialists, Inc., 204 Andover St., Andover, MA 01810
66. A. J. L. Hutchinson, The Ben Holt Co., 201 South Lake Ave., Pasadena, CA 91101
67. R. K. Iler, 311 Haines Ave., Wilmington, DE 19809
68. M. Kastner, Scripps Institute of Oceanography, PO Box 1529, La Jolla, CA 92037
69. S. Kitahara, Fukuoka University of Education, Akama, Munakota, Cho, Fukuoka-ken, 811-41, JAPAN
70 G. A. Kolstad, DOE, Washington, DC 20545
71. R. F. Krueger, Union Oil Research Center, PO Box 76 Brea, CA 92621
72. P. LaMori, EPRI, PO Box 10412, Palo Alto, CA 94303
73. A. S. López, Universidad Autonoma, Metropolitana-Iztapolapa, Departmento de Ingeniería, Apartado Postal 55-534, MEXICO 13, D. F.
74. R. L. Macy, Suntech Inc., 503 N. Central Expressway, Richardson, TX 75080

75. W. A. J. Mahon, Chemistry Div., D.S.I.R., c/o M.O.W., P.B. Taupo, NEW ZEALAND
76. L. Mahone, Dow Corning Corp., MS 54, South Saginaw Rd., Midland, MI 48640
77. A. C. Makrides, EIC Corp., 55 Chapel St., Newton, MA 02158
78. C. McFarland, DOE, Div. of Geothermal Energy, Washington, DC 20545
79. R. McKay, Jet Propulsion Laboratory, 4800 Oak Grove Drive, Pasadena, CA 91103
80. S. Mercado, Federal Commission of Electricity, Melchor Ocampo No. 455-5° piso, MEXICO 5, D. F.
81. S. J. Moore, Carrier Corp., Research Div., Carrier Parkway, Syracuse, NY 13066
82. C. B. Moyer, Acurex Aerotherm, Technology Dept., 485 Clyde Ave., Mountain View, CA 94042
83. P. Muffler, U. S. Geological Survey, 345 Middlefield Road, Menlo Park, CA 94025
84. P. B. Needham, U. S. Dept. of Interior, Bureau of Mines, College Park, MD 20740
85. D. L. Nielson, University of Utah Research Institute, Earth Science Lab., 391-A Chipeta Way, Salt Lake City, UT 84106
86. L. B. Owen, LLL, PO Box 808, L-224, Livermore, CA 94550
87. H. Hunter Paalman, Dow Chemical Research Laboratories, 2800 Mitchell Drive, Walnut Creek, CA 94598
88. J. Perona, University of Tennessee, Chemistry Dept., Knoxville, TN 37916
89. S. Phillips, LLL, PO Box 808, Livermore, CA 94550
90. H. P. Poppendiek, Geoscience Ltd., 410 S. Cedros Ave., Solana Beach, CA
91. H. Recht, Atomics International, 8900 DeSoto Ave., Canoga Park, CA 91304

92-94. R. R. Reeber, DOE, 20 Massachusetts Ave., NW, Washington, DC 20545

95. R. W. Rex, Republic Geothermal Inc., 11823 E. Slauson Ave., Santa Fe Springs, CA 90670
96. H. P. Rothbaum, Chemistry Div., Dept. of Scientific Research, Private Bag, Petone, NEW ZEALAND
97. R. K. Sapre, Central Salt and Marine Chemicals Research Institute, Waghawadi Road, Bhaunagar-364002, INDIA
98. R. Sears, Lockheed, PO Box 1103, Huntsville, AL 35807
99. M. A. Selim, Asst. Technical Director, Core Laboratories, Inc., PO Box 47547, Dallas, TX 75247
100. D. W. Shannon, Battelle Northwest Laboratory, Battelle Blvd., Richland, WA 99352
101. E. F. Slattery, Facilities Systems Engineering Corp., 8332 Osage Ave., Los Angeles, CA 90045
102. L. B. Smith, DOE, Tech. Information Center, PO Box 62 Oak Ridge, TN 37830
103. R. S. Sprankle, Hydrothermal Power Co., Ltd., 27032 Via Callado, Mission Viejo, CA 92675
104. W. J. Subcasky, Chevron Oil Field Research , PO Box 446, La Habra, CA 90631
105. B. C. Syrett, Stanford Research Institute, Ravenwood Ave., Menlo Park, CA 94025

106. G. Tardiff, LLL, PO Box 808 Livermore, CA 94550
107. J. Tester, LASL, PO Box 1663, Los Alamos, NM 87545
108. A. P. Thiruvengadam, Daedalean Associated, Inc., 15110 Springlake Research Center, Woodbine, MD 21797
109. P. Tipping, Research Library, Texasgulf, Inc., 200 Park Ave., New York, NY 10017
110. H. Van Baldwin, Research Triangle Institute, EER Div., Box 12194, Research Triangle Park, NC 27709
111. N. J. Van Sickels, The Rust Engineering Co., 1130 South 22nd St., PO Box 101 Birmingham, Al 35201
112. O. Vetter, Vetter Research, 3189-C Airway Ave., Costa Mesa, CA 92626
113. K. L. Wagner, Allied Chemical Corp., 550 Second St., Idaho Falls, ID 83401
114. E. F. Wahl, Occidental Petroleum Research Laboratory, 1855 Carrion Road, LaVerne, CA 91750
115. O. Weres, LBL, Berkeley, CA 94720
116. L. Werner, DOE, Washington, DC 20545
117. W. R. Wilcox, Clarkson College of Technology, Dept. of Chemical Engineering, Potsdam, NY 13676
118. J. S. Wilson, Dow Chemical Co., Bldg. A-1205, Freeport, TX 77541
119. P. Witherspoon, LBL, Berkeley, CA 94720
120. Assistant Manager, Energy Research and Development, DOE-ORO
121-297. Given Distribution as shown in TID 4500, UC-4 Chemistry

☆U.S. GOVERNMENT PRINTING OFFICE: 1980-640-245-417